Field Determination of Optimal Dates for the Discrimination of Invasive Wetland Plant Species Using Derivative Spectral Analysis

Magdeline Laba, Fuan Tsai, Danielle Ogurcak, Stephen Smith, and Milo E. Richmond

Abstract

*Mapping invasive plant species in aquatic and terrestrial ecosystems helps to understand the causes of their progression, manage some of their negative consequences, and control them. In recent years, a variety of new remote-sensing techniques, like Derivative Spectral Analysis (DSA) of hyperspectral data, have been developed to facilitate this mapping. A number of questions related to these techniques remain to be addressed. This article attempts to answer one of these questions: Is the application of DSA optimal at certain times of the year? Field radiometric data gathered weekly during the summer of 1999 at selected field sites in upstate New York, populated with purple loosestrife (*Lythrum salicaria L.*), common reed (*Phragmites australis (Cav.)*) and cattail (*Typha L.*) are analyzed using DSA to differentiate among plant community types. First, second and higher-order derivatives of the reflectance spectra of nine field plots, varying in plant composition, are calculated and analyzed in detail to identify spectral ranges in which one or more community types have distinguishing features. On the basis of the occurrence and extent of these spectral ranges, experimental observations suggest that a satisfactory differentiation among community types was feasible on 30 August, when plants experienced characteristic phenological changes (transition from flowers to seed heads). Generally, dates in August appear optimal from the point of view of species differentiability and could be selected for image acquisitions. This observation, as well as the methodology adopted in this article, should provide a firm basis for the acquisition of hyperspectral imagery and for mapping the targeted species over a broad range of spatial scales.*

Introduction

The invasion of aquatic and terrestrial ecosystems by non-indigenous plant and animal species is causing extensive environmental and economic damage through habitat change and loss. Whether intentionally or accidentally introduced, these species often negatively impact the integrity, function, and productivity of many ecosystems by disrupting a number of physical, chemical, and biological processes inherent in these systems (Thompson *et al.*, 1987; Stein and Flack, 1996). In recent years, the disturbance caused to a wide range of ecosystems has brought about significant concern and led to a sizeable research effort.

Part of that effort has consisted of mapping the progression of invasive species through time in various geographical regions. These maps enable researchers to monitor the status of the invasion and provide information in a format suitable to educate decision makers or the public, and to alert them of looming problems (for example, Byers *et al.*, 2002). They also serve the needs of various stakeholders who may benefit from knowing the status of an invasive plant in the landscape.

One of the most popular methods of gathering spatially-distributed data on invasive species vegetation is through remote sensing techniques. Aerial imagery has been extensively used, with most documented studies using large-scale (1:5000 to 1:10 000) aerial photography of the landscape during key growing seasons (Armstrong, 1979; Frazier and Moore, 1993; McCormick, 1999; Holroyd and Eberts, 2000). Digital satellite imagery, e.g., Landsat Thematic Mapper (TM), and color infrared photography have been the traditional sources of data (Everitt *et al.* 1995; Hanlon, 1995; Rowlinson *et al.* 1999). More recently, hyperspectral imagery has been used to map invasive species (Bachmann *et al.*, 2002; Williams and Hunt, 2002; Hirano, 2003)

In principle, because of their large number of wavebands (224) and narrow (10 *n*m) bandwidths, hyperspectral remotely-sensed data provide researchers the opportunity to pursue complex analysis that might be difficult to carry out using traditional multispectral data (e.g., Underwood *et al.*, 2003). However, until a decade ago, practical applications of hyperspectral information were hindered by a number of daunting challenges (Tsai and Philpot, 2002). Among these were having to deal with larger data volumes and correspondingly longer processing times than in multispectral analyses. Another, possibly more substantive challenge, was to make effective use of the new information obtained from the data. Fortunately, these obstacles have been surmounted to a large extent over the last few years, and several methods now exist to effectively select spectral features from hyperspectral data sets. Some approaches used include the calculation of

M. Laba, D. Ogurcak and S. Smith are with the Institute for Resource Information Systems, Department of Crop and Soil Sciences, Rice Hall, Cornell University, Ithaca, New York 14853 (ml49@cornell.edu).

F. Tsai is with the Center for Space and Remote Sensing Research, National Central University, Zhong-Li, Taoyuan 320, Taiwan, China.

M. Richmond is with the USGS New York Cooperative Fish and Wildlife Research Unit, Fernow Hall, Cornell University, Ithaca, New York 14853, USGS-BRD.

Photogrammetric Engineering & Remote Sensing
Vol. 71, No. 5, May 2005, pp. 603–611.

0099-1112/05/7105–0603/$3.00/0

band moments (Staenz, 1996), orthogonal subspace projection (Harsanyi and Chang, 1994), band prioritization and decorrelation (Chang *et al.*, 1999), and the minimum noise fraction transform (Green *et al.*, 1988; Lee *et al.*, 1990). Although conceptually very different, these methods all aim to reduce the dimensionality of the spectral domain with minimal loss of useful information. However, a potential danger with all of these approaches is the loss of important spectral information, particularly if the spectral details of interest exhibit a small variance relative to other features in the data set (Tsai and Philpot, 2002). This danger is in principle alleviated, or at least diminished, in Derivative Spectral Analysis (DSA).

The conceptual basis of DSA is that, if hyperspectral data are more than just a large number of bands from which one may choose an optimal subset, the unique information will be in the relative change of adjacent bands, i.e., in the shape of the spectra (Tsai and Philpot, 2002). Since derivatives characterize the shape of a curve, they are likely candidates for the capture of spectral details that would be lost by other methods (Demetriades-Shah *et al.*, 1990). In addition, because it focuses on the shape rather than the amplitude of spectra, DSA does not necessarily require independent reference spectra, nor is it sensitive to differences in illumination intensity, whether caused by changes in sun angle, cloud cover, or topography.

DSA has been shown to be an effective method to identify subtle features from hyperspectral data sets (Tsai and Philpot, 1998), has been used in coastal environmental studies (Philpot *et al.*, 1997; Philpot and Kohler, 1999; Clark *et al.*, 2000) and has been extended to classify hyperspectral data for land cover applications (Tsai and Philpot, 2002). DSA has been used to analyze unusual spectral features and to construct a yellowness index for vegetation stress studies (Philpot *et al.*, 1996; Adams *et al.*, 1999). It has also been used to identify subtropical tree species (Fung *et al.*, 2000) and to classify vegetation in a wetland environment (Qingxi *et al.*, 1997).

To date, DSA has not been used in any invasive species mapping or detection project, and a number of key questions related to its application in this context have yet to be addressed. Foremost among them is whether, in using DSA for the purpose of mapping invasive plant species, some dates of the year are preferable than others, i.e., lead to easier or more accurate differentiation among plant community types. An economical way of answering this question is to acquire and analyze field measurements, instead of remotely-sensed data, to narrow the time window suitable for the application of DSA.

In this general context, the key objective of this article is to describe and test a procedure, based on field spectroradiometer measurements, that identifies optimal dates for the application of DSA to the discrimination and, eventually, to the mapping of invasive plant species. This article focuses on three field sites in upstate New York, each dominated by one of three targeted plant species. Two of them, purple loosestrife (*Lythrum salicaria*) and common reed (*Phragmites australis*) are on the "Top 20 Invasive Plant Species" list prepared by the Invasive Plant Council of New York State (IPC of NYS, 2005), and are considered two of the most widespread and damaging plant invaders in temperate North American wetlands (Spencer, 1999). The third plant species considered in this paper is cattail (*Typha spp.*). First, second and higher-order derivatives of the reflectance spectra of nine field plots, varying in plant composition, are calculated and analyzed in detail to identify spectral ranges in which one or more community types have distinguishing features. Based on the occurrence and extent of these spectral ranges, we determine which dates are optimal for species differentiability. Attempts are then made to assess whether these optimal dates coincide with specific growth stages or phenology changes of the plants, whose occurrence can be monitored in the field.

Methods

Field Measurements

A two-step field sampling and characterization methodology was designed and implemented during the field season of 1999. For the purposes of this study, we chose to follow the New York State Freshwater Wetlands Inventory System of community type identification (Cole and Fried, 1981) and defined a species-dominated plant community as one with greater than two-thirds average cover by the dominant plant over the area occupied by the plant community. Visual estimation of percent cover at the canopy level was used to locate, in upstate New York (Figure 1), representative field sites for each of the three invasive plants of interest (purple loosestrife, reed, and cattail). At each site, three 2.74 m by 2.74 m sample plots were selected to capture the variability of species composition (richness and diversity) due to site characteristics. In each case, small understory vegetation was growing mostly underneath plants of the dominant species (purple loosestrife, reed, or cattail). Therefore, stem counts were used at the plot scale to insure that the understory vegetation was accounted for accurately in the assessment of plant diversity.

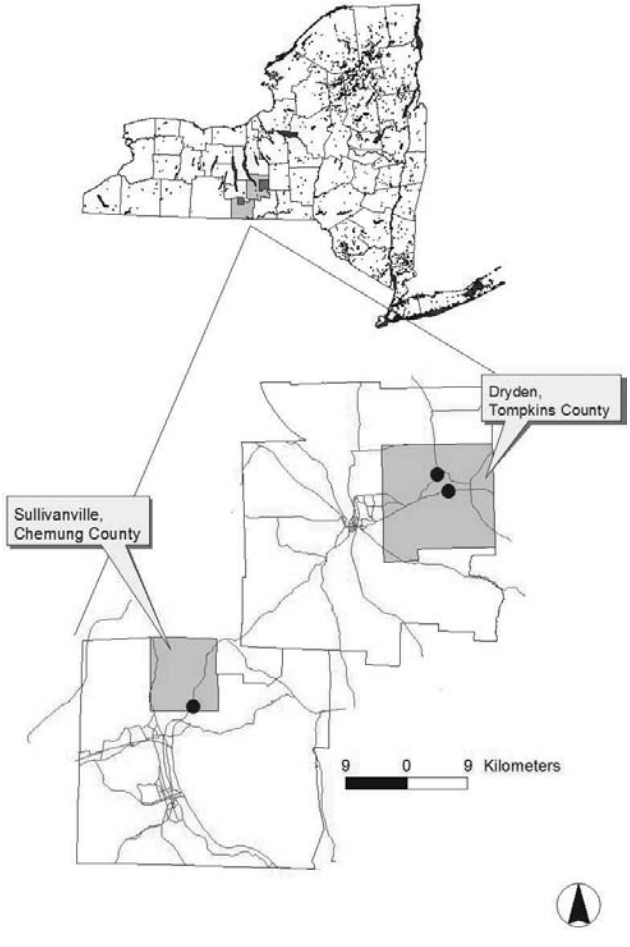

Figure 1. Location of the three wetland sample sites in upstate New York.

Plant composition at each site (Table 1) was described following Tiner (1987), and Gleason and Cronquist (1991).

Radiometric measurements were made once a week on the same, tagged plants within the sample plots for the duration of the experiment. Measurements began during the last week of June and continued until the first frost, on 15 October. An Ocean Optics dual channel SD1000 miniature fiber optic spectroradiometer was used to measure *in situ* reflectance characteristics of the sample plots at each field location. The SD1000 is a compact, portable spectroradiometer that uses a diffraction grating (600 lines at 750 *n*m) to disperse the incoming light onto a silicon photodiode array with a 50 μm slit and a GC475 filter. The SD1000 measures radiance from 500 *n*m to 1000 *n*m with an effective bandwidth of approximately 5 *n*m. The spectroradiometer was interfaced with an OOIbase™ software package on a notebook computer through a DAQCARD-700 PCMIA-type *A/D* card (Ocean Optics,[1] Inc., 2005). This instrument and associated software are designed to perform five successive measurements automatically within a few seconds of each other. The mean of these five measurements yields an average spectrum, which serves as a basis for the computation of derivatives.

Reflectance of a plant is calculated using simultaneous measurements of both the plant itself (target) and a reference material with known spectral properties. For additional calibration, dark current and standard measurements were made of both sensors at the beginning and end of each sitting.

The sensor for the plants has a 14° field of view. At 30 cm above the plant, this translates into a 15 cm diameter measurement window. For this study, the sensor was mounted on a pole and held approximately 30 cm above a plant that, with leaves, seed heads, or flowers included, was greater than or equal to 15 cm in diameter. All measurements were taken at 0° (nadir). The protocol was to make one measurement at each of the three plots at each location in the afternoon of the same day. Measurements were not taken if the wind caused the sensor to move appreciably off-nadir or if the sky became significantly overcast. In these cases, measurements were resumed on the next available day.

The resulting spectra were influenced mostly by the plants above which the sensor was positioned. However, the spectra were also affected by site characteristics including understory vegetation, standing water, or the underlying soil.

TABLE 1. PLANT COMPOSITION OF SAMPLE PLOTS FOUND IN TOMPKINS AND CHEMUNG COUNTIES, NEW YORK. PLANTS OCCUPYING LESS THAN 10 PERCENT OF THE PLOT HAVE BEEN OMITTED FROM THE TABLE.

Cattail meadow, Dryden, Data Collection, 01 July 1999			
	Common Name	Scientific Name	Percent Cover*
Plot #1	Narrow-leaved Cattail	*Typha angustifolia*	80
	Forget-me-not	*Myosotis scorpioides*	10
	Spotted Touch-me-not	*Impatiens capensis*	10
Plot #2	Narrow-leaved Cattail	*Typha angustifolia*	70
	Spotted Touch-me-not	*Impatiens capensis*	20
	Wide-leaved Sedge	*Carex sp.*	10
Plot #3	Narrow-leaved Cattail	*Typha angustifolia*	60
	Wide-leaved Sedge	*Carex sp.*	20
	Spotted Touch-me-not	*Impatiens capensis*	10
	Other		10
Purple loosestrife meadow, Dryden, Data Collection, 01 July 1999			
	Common Name	Scientific Name	Percent Cover*
Plot #1	Purple loosestrife	*Lythrum salicaria*	50
	Sedge	*Carex sp.*	20
	Soft rush	*Juncus effusus*	10
	Redtop	*Agrostis gigantea*	10
	Goldenrod	*Solidago sp.*	10
Plot #2	Purple loosestrife	*Lythrum salicaria*	70
	Redtop	*Agrostis gigantea*	10
	Sedge	*Carex sp.*	10
	Soft rush	*Juncus effusus*	10
Plot #3	Purple loosestrife	*Lythrum salicaria*	40
	Goldenrod	*Solidago sp.*	40
	Redtop	*Agrostis gigantea*	10
	Sedge	*Carex sp.*	10
Reed meadow, Sullivanville, Data Collection, 15 July 1999			
	Common Name	Scientific Name	Percent Cover*
Plot #1	Reed	*Phragmites communis*	70
	Redtop	*Agrostis gigantea*	30
Plot #2	Reed	*Phragmites communis*	70
	Redtop	*Agrostis gigantea*	10
	Sedge	*Carex sp.*	10
	Blue vervain	*Verbena hastate*	10
Plot #3:	Reed	*Phragmites communis*	80
	Bunch or Cut grass	*Gramineae*	5
	Sedge	*Carex sp.*	5
	Other		10

*Percent cover is based on stem density measurements.

Data Analysis

Graphs of relative reflectance of purple loosestrife versus wavelength were produced from the field spectra. Absolute reflectance is given by the expression:

$$\text{Relative reflectance} = \frac{(\text{Target radiance} - \text{Dark radiance})}{(\text{Standard radiance} - \text{Dark radiance})}. \quad (1)$$

Target, dark, and standard radiance values were calculated from the average of the five measurements taken at each sitting.

We computed derivatives of different orders and at different band separations (sampling intervals) of our field spectra using several computational modules developed in MATLAB (Mathworks, 2005) that are collectively known as HYPERSPEC (Tsai and Philpot, 1998) and that are available from the corresponding author upon written request. Iterative examinations of the data resulted in the fine-tuning of a number of parameters (methods for smoothing, filter size, band separation) to optimize noise reduction and adjust the effective sampling interval to match the scale of the spectral features of interest. A mean-filter, smoothed finite approximation algorithm was selected to examine the first to fifth order derivatives.

Smoothing or otherwise minimizing random noise, of the original spectra is necessary because derivatives are notoriously sensitive to noise. Several options are available to smooth data, such as the Savitzky-Golay and the Kawata-Minami's smoothing algorithms (e.g., Tsai and Philpot, 1998). The "mean filter" algorithm was selected in the present work, in part because it is the most straightforward to use and requires the least amount of computational effort. Such an algorithm also has been shown to work well whenever the spectral features of interest are larger than the selected filter size (Tsai and Philpot, 1998). This smoothing algorithm simply replaces the value of the spectrum at a given wavelength by

[1]Mention of commercial products or trade names does not imply endorsement by the U.S. Government.

the mean spectral value of all points within a specified window centered at that wavelength, following the equation:

$$\hat{s}(\lambda_j) = \frac{\sum s(\lambda_i)}{n} \tag{2}$$

where n (number of sampling points) is the filter width and j is the index of the middle point of the filter.

After smoothing of the data, derivatives can be calculated in a number of ways, for example by fitting a polynomial or cubic spline to the spectrum, and deriving analytically the resulting equations. However, experience has shown that a simple, numerical estimation procedure is equally effective. Finite approximation can be used to estimate derivatives by suitable difference schemes with a finite band resolution, $\Delta\lambda$. In this study, following Tsai and Philpot (1998, 2002), the first derivative is estimated by:

$$\left.\frac{ds}{d\lambda}\right|_i \approx \frac{s(\lambda_i) - s(\lambda_j)}{\Delta\lambda} \tag{3}$$

where $\Delta\lambda$ is the separation between adjacent bands, $\Delta\lambda = \lambda_j - \lambda_i$ and $\lambda_j > \lambda_i$, and the sampling interval can be calculated dynamically using sample wavelengths across spectra. The second derivative can be derived from the first derivative as follows:

$$\left.\frac{d^2s}{d\lambda^2}\right|_j = \frac{d}{d\lambda}\left(\frac{ds}{d\lambda}\right)\Bigg|_j \approx \frac{s(\lambda_i) - 2s(\lambda_j) + s(\lambda_k)}{(\Delta\lambda)^2} \tag{4}$$

where $\Delta\lambda = \lambda_k - \lambda_j = \lambda_j - \lambda_i$, $\lambda_k > \lambda_j > \lambda_i$.

In the same fashion, higher-order derivatives are computed iteratively, and any order of derivative is accessible using the finite approximation. In general, the nth derivative is computed as

$$\left.\frac{d^ns}{d\lambda^n}\right|_j = \frac{d}{d\lambda}\left(\frac{d^{(n-1)}s}{d\lambda^{(n-1)}}\right)\Bigg|_j = \cdots \approx \frac{s(\lambda_i) - \cdots + s(\lambda_{i+n})}{(\Delta\lambda)^n} = \frac{\sum_i^{i+n} C_k s(\lambda_k)}{(\Delta\lambda)^n} \tag{5}$$

where $j = (2i + n)/2$, if $(2i + n)$ is even, or $j = (2i + n + 1)/2$, if $(2i + n)$ is odd. This means that if the position of the resultant derivative falls between sampling points, it is assigned to the sampling point at the next larger wavelength or wave number. The coefficients C_k are calculated using an iteration scheme.

In the calculations, a "boxcar" approach (Tsai and Philpot, 1998) was used, which consists of taking the same value for the size (bandwidth) of the smoothing filter and for the band separation used in the computation of the derivatives. We determined empirically, in successive trials, that the value of 21 was optimal.

Results and Discussion

The reflectance spectra and the first to fifth derivatives of the plant radiance spectra at each measurement date were compared to assess spectral differentiability among purple loosestrife, reed, and cattail. We looked for differences in magnitude and slope, passage through zero of some of the curves, differences in the sign (positive or negative) of the derivative values, and, generally, regions where all the curves, or at least some of them, exhibited distinct behaviors. This comparison could in principle be carried out automatically using a computational module written in MATLAB for this specific purpose. However, since in the context of our preliminary analysis of the feasibility of species detection using DSA, we were interested in clearly noticeable trends in the data, visual comparison of the curves was deemed sufficient. Application of this procedure is described in the following for the arbitrarily selected spectra obtained on 23 September.

The original reflectance spectra (Figure 2) associated with the different community types exhibit similar features, with inflections and extremas occurring at roughly the same wavelengths and with an increase in reflectance at the "red edge", around 700–750 *n*m. Reflectivity in the visible spectrum range (450–750 *n*m) is typical of senescing plants and a mix of dry and green vegetation. The characteristic peak-and-valley configuration associated with chlorophyll production in healthy green vegetation is absent from the spectra. Instead, the curves suggest a decrease in chlorophyll absorption in the blue and red bands, and an increase in red reflectance. For purple loosestrife, this combination of red and green reflectance indicates that leaves are becoming increasingly yellow and red. For cattail, this behavior of the spectra can be explained by the presence of brown remnants of previous year's plants (Juan and Shih, 1997; Juan *et al.*, 2000). Differences between red and NIR reflectance are relatively low in the reflectance spectra of all three plants due to their vertical canopy structure (Spanglet *et al.*, 1998). In the near-infrared region, purple loosestrife has a relatively low reflectance, which may be due to its dry brown seedpods and senescing leaves, to interspersed browning grasses, and to effects of the underlying soil (Spanglet *et al.*, 1998). On the other hand, the densely planted cattail has a comparatively high reflectance in the near-infrared region, probably because its leaves are still mostly green.

Standard errors associated with the various curves in Figure 2 (and in subsequent figures as well), are generally too small to be represented in the graphs. For example, the average standard deviations associated with the three curves for the loosestrife-dominated plots in Dryden, in the range of wavelengths depicted in Figure 2 are 0.006, 0.004, and 0.015, respectively for plots No. 1, No. 2 and No. 3.

In Figure 2, the reflectance spectra associated with the cattail- and loosestrife-dominated community types are distinct. The fact that reed does not follow the same pattern makes it impossible to use reflectance values to distinguish reed from the other community types, at least on 23 September. Further community type identification could be achieved based on slight differences in slope or concavity in the original spectra (Tsai and Philpot, 1998; 2002). One of the basic tenets of derivative analysis is that these differences appear much more clearly in graphs of first or higher-order derivatives. A second tenet is that these derivatives

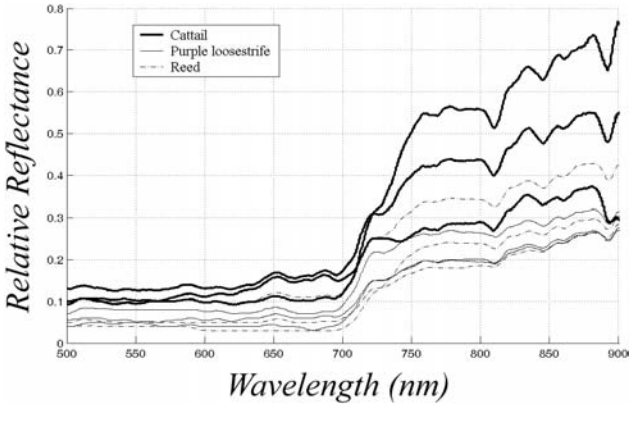

Figure 2. Average reflectance spectra of three wetland communities, acquired on 23 September 1999. (n = 5).

can be computed based on the untransformed radiance spectra, obviating the need to compute reflectance.

As in the reflectance spectra, the first derivative of the radiance curves (Figure 3), associated with the different community types have similar features, with inflections and extremas occurring at roughly the same wavelengths. Occasionally, some slight difference may be used to distinguish curves. For example, at a wavelength of 670 *n*m, the curves for cattail exhibit a relative minimum, whereas the curves for purple loosestrife and reed do not. In general, however, behavioral differences between curves are too small to serve as diagnostic criteria. Fortunately, in a number of ranges of wavelengths, the location of the curves in the graph can be used to distinguish one curve or set of curves from the others (indicated by arrows in Figure 3). For example, at several wavelengths, the curve for reed Site No. 3 lies clearly below those for the other two reed plots, as well as those for the cattail and purple loosestrife community types.

In the graph of the second derivatives (Figure 4), reed Site No. 3 again has a very distinct behavior, with significantly deeper minima and higher maxima, relative to the other community types at a number of wavelengths (indicated by arrows in Figure 4a). In two ranges of wavelength (670–685 *n*m and 685–702 *n*m), purple loosestrife Sites 1 and 2 are also distinguishable as they are at mid-distance between the curve for reed Site No. 3 and all the other curves (Figure 4b). At a wavelength of 965 *n*m, purple loosestrife Site No. 1 has a small but clear relative minimum, in contrast with the other curves for loosestrife and for the other community types, which exhibit a relative minimum at a slightly lower wavelength, around 955 *n*m.

The graph of the third derivatives (Figure 5) exhibits many of the same features as that of the second derivatives, with reed Site No. 3 again having a very distinct behavior over many ranges of wavelength. Its curve is markedly higher or lower than the other curves. In two ranges of wavelength (675–695 *n*m and 700–710 *n*m), purple loosestrife Sites No. 1 and No. 2 are also distinguishable as they are at mid-distance between the curve for reed Site No. 3 and all the other curves (Figure 4).

The preceding analysis of the first, second, and third derivatives yields a number of wavelength intervals, or windows, in which one or more community types have distinguishing features that potentially could be used to distinguish them. Higher-order derivatives did not provide additional insight and are not mentioned further in the following analyses. In some cases, the identified intervals overlap entirely. This is the case, for example, with the 740 *n*m–750 *n*m intervals for reed Site No. 3 in both Figures 3 and 5. In other cases, the intervals overlap only partially, but

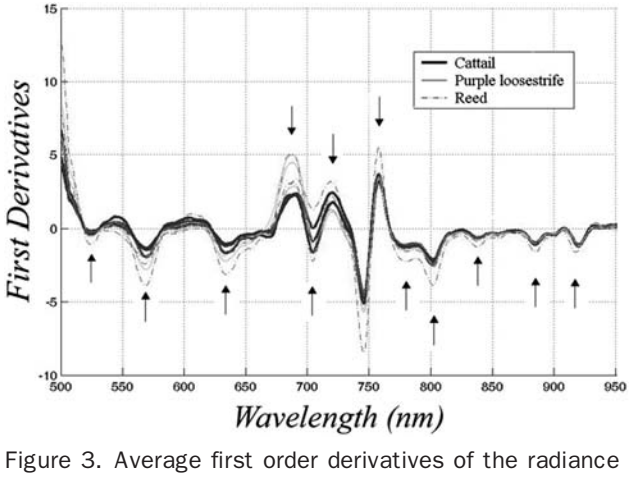

Figure 3. Average first order derivatives of the radiance spectra of three wetland communities, acquired on 23 September 1999. (n = 5).

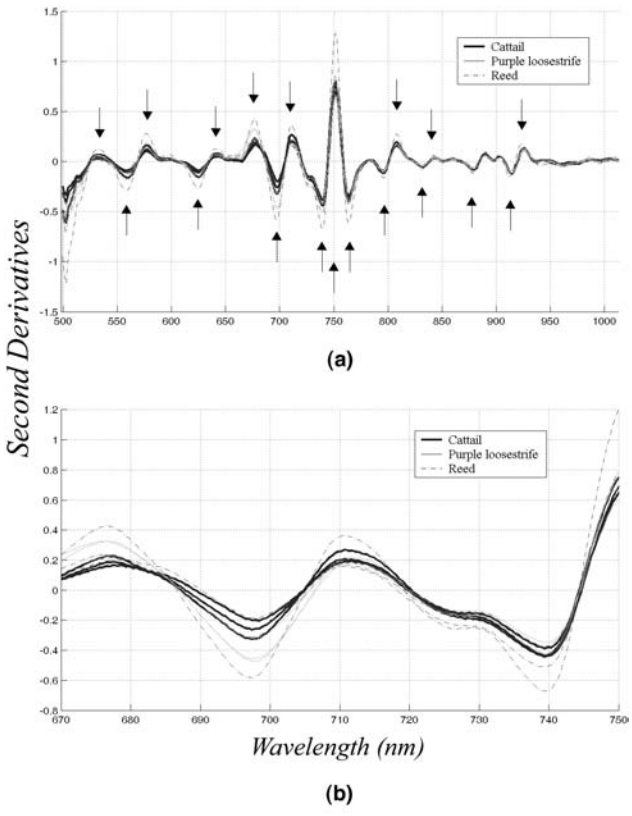

Figure 4. Average second order derivatives of the radiance spectra of three wetland communities, acquired on 23 September 23. (n = 5): (a) reed Site No. 3, (b) purple looseleaf Sites No. 1 and No. 2.

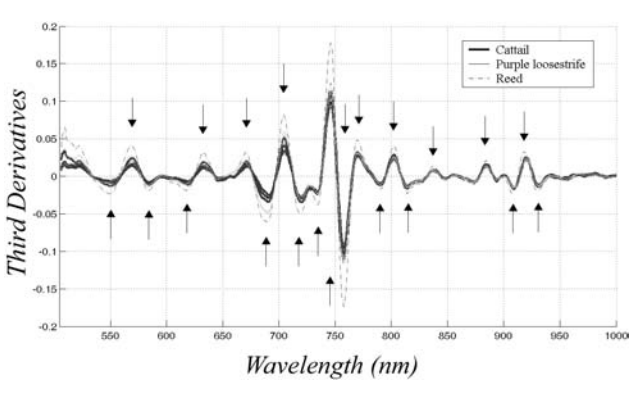

Figure 5. Average third order derivatives of the radiance spectra of three wetland communities, acquired on 23 September 1999. (n = 5): (a) reed Site No. 3, (b) purple loose leaf Sites No. 1 and No. 2.

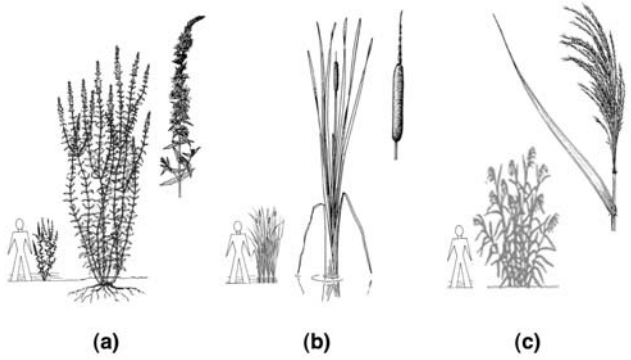

Figure 6. Schematic illustration of the morphology and growth forms of (a) purple loosestrife (*Lythrum salicaria*.), (b) cattail (*Typha spp*.) and (c) common reed (*Phragmites australis*). Note: Modified from http://www.npwrc.usgs.gov/resource/1999/loosstrf/field.htm, http://aquat1.ifas.ufl.edu/lytsaldr.jpg, http://aquat1.ifas.ufl.edu/typha2.jpg, http://aquat1.ifas.ufl.edu/phraus2.jpg (last date accessed: 22 February 2005).

are clearly associated with the same spectral feature. For example, the two windows at 740 *n*m–750 *n*m and 755 *n*m–760 nm for reed Site No. 3 in Figure 5 are associated with the rising and descending parts of a peak centered at 750 *n*m, and roughly extending from 746 *n*m to 755 *n*m, in the reed Site No. 3 curve in Figure 4. Adoption of this perspective allows us in Table 2 to summarize the comparison results in a convenient manner, by omitting the often-redundant information provided by the second and higher-order derivatives. For a few dates, analysis of the higher-order derivatives reveals the existence of additional windows, for example 668 *n*m–690 *n*m for purple loosestrife Site No. 2 on 12 August, in which discrimination of one or more community types is possible.

The information summarized in Table 2 allows us to determine which date is optimal for community type discrimination. We are looking for a date for which the individual community types ("reed", "cattail", and "purple loosestrife") are all distinguishable. A complementary criterion that could be used to determine how optimal specific dates are would be the number of spectral ranges in which community type differentiability is manifested at a given date. The larger the number of usable spectral ranges, the easier it would be to map the given area.

Six dates, 15 July, 29 July, 05 August, 30 August, 03 September, and 30 September, afford good discrimination among community types. At least one and often two plots can be identified for each individual community type. On 30 August, the spectra allow full differentiability for the community types. In the spectral range 680 *n*m to 740 *n*m, the first-derivative curves associated with the reed, cattail, and purple loosestrife community types can be distinguished from each other, i.e., the three reed curves are distinct from the three cattail curves and the three purple loosestrife curves.

The fact that an interval near 700 *n*m turns out to be optimal for the discrimination of the targeted wetland plants is hardly a surprise. Numerous authors have found the part of the light spectrum near the "red-edge" to be very sensitive to slight differences in plant morphology or in their immediate environment (soil type, hydric conditions), and therefore to be very useful to discriminate among various plant community types (Spanglet *et al.*, 1998; Nellis and Tao, 1999; Fung *et al.*, 2001; Thenkabail *et al.*, 2002; Splajt *et al.*, 2003)

The fact that optimal dates occur during August is not entirely surprising either, given the differences in the phenological stages of the three plants. In a purple loosestrife plant, up to 50 herbaceous stems rise from a common rootstock to produce a characteristic, graceful, wide-topped crown. Purple loosestrife has a long season of bloom (from late June to early September in most areas). In 1999, it started blooming in the middle of July and the majority of buds were in full bloom, with a characteristic reddish-purple color, by early August. By 12 August, most stems were beginning to lose their flower masses, from the bottom of the stems upwards, and the process was almost complete by the beginning of September, with a progressive change of color from purple to brown, accentuated by the presence of brown seed heads. Concomitantly, a number of other plants appeared and started blooming in the purple loosestrife plots, including goldenrod (*Solidago sp*.) and chicory (*Cichorium intybus*).

Reed has a different phenology, characterized by a towering height of up to four meters (approximately 14 feet), stiff wide leaves, and hollow stems. Its feathery and drooping inflorescences (clusters of tiny flowers) that grow at the tops of the stems are purplish when flowering and turn whitish, grayish, or brownish when in fruit. A typical inflorescence may be one to two feet long, and several inches wide. They drape to one side and wave like plumes in the breeze. At the field sites, blooming started later than for purple loosestrife, around 05 August. By 09 September, seed heads had turned from purple to brown. Later in the month, reed plants exhibited brown to whitish tassels, on top of stems with an average height of about 225 cm.

Cattail plants typically bloom in June and July. By the end of August, all that remains of the male-female inflorescences is the brown, cylindrical flower spikes, up to one foot long, that give the cattail its name and resemble a "sausage-on-a-stick". The stems are dark brown with an average height of about 210 cm. They are surrounded by flat, sheathing, pale, or grayish-green, leaves that remain somewhat uniformly green during August and September.

Based on this phenological information (Figure 6), it would seem that in terms of differentiability between plant species, August would be a good candidate month. During that month, indeed, tall reed plants harboring purple inflorescences, progressively replaced by brownish/whitish tassels, freely moving in the wind, provided a sharp contrast to the shorter plants that were either uniformly green (cattail, with vertically oriented stems and flowers) or purple loosestrife with brown seed heads (also more consistently oriented vertically, and therefore presenting less of a foot print to field sensors placed vertically above the plants, or to satellite-based cameras). By contrast, in early October, cattail and reed plants turned brown, while purple loosestrife plants turned reddish, providing overall less opportunity to differentiate between species.

Conclusions

The key objective of this article was to describe and test a procedure, based on field spectroradiometer measurements, that identifies optimal dates for the application of DSA to the discrimination of invasive plant species. This procedure was tested on three field sites in upstate New York, each dominated by one of three targeted plant species; purple loosestrife (*Lythrum salicaria L*), common reed (*Phragmites australis*) and cattail (*Typha spp*.). First, second and higher-order derivatives of the reflectance spectra of nine field plots, varying in plant composition, were calculated and analyzed

TABLE 2. WAVELENGTHS FOR COMMUNITY TYPE DISCRIMINATION WITHIN THE FIRST, SECOND, AND THIRD DERIVATIVES BY DATE, DOMINANT PLANT SPECIES, AND PLOT NUMBER. THE NUMBERS IN PARENTHESES CORRESPOND TO PLOTS THAT CAN BE DISCRIMINATED AT A GIVEN WAVELENGTH.

Date (1999)	Plant	Plot	First Derivative Wavelength (*n*m)	Second Derivative Wavelength (*n*m)	Third Derivative Wavelength (*n*m)
06-July	reed	2	500–670, 680–730,745–770, 780–880,920–935,970–1025		
	cattail	1 & 2	685–700,815–820,840–845, 865–875,922–934,965–975	965–975	
15-July	reed	1	523–536,550–570,610–625, 666–685,695–700,940–970		
	reed	2	540–550,570,610,620, 640,665,950–995		
	cattail	2	555–575		
	pl	1	510–550,637–645,685–710,750		
22-July	reed	1 & 3	550–570(1),595–620(1),670–685(1), 705–725(1),782–797(3),880(1), 870–880(3),897–915(3),905(1), 955–960(1)	907	
	pl	1,2,3	560–585(2), 685–715		
29-July	reed	1& 3	510–525(1),540–545(1,3),585(1), 592–670(1,3), 677–740(3)		
	cattail	1 & 3	525–535,750–765,765–775,780–940		
	pl	1 & 3	540–545(3),595–635(3),600–605(1), 658(3),665(3),690–725(3),755(3)	600–605(1)	
05-August	reed	1 & 3	528–547(1),530(3),553–572(1),555(1,3), 560–580(3), 680–680(1),705–740(1), 750(3),955–965(1)		
	cattail	1	555		
	pl	3	590–635(1,3),665(3),690(3)	604(1)	
12-August	reed	1 & 2	545(1),550(2),565(1,2),700(1,2),710(1,2), 730(1,2),750(3),655–668(1),766–776(3)		
	pl	2	668–690		668–690
30-August	reed	2 & 3	750–775(2,3)		572–588(1),720–728(3)
	cattail	3	565–592,705–720,720–740		
	pl	1 & 3	500–550(1),570–590(1),630–645(1,3), 650–660(1,3),690–710(1,3),735(1), 740(3),765–775(1,3)		
	all 3		680–740		
03-September	reed	1 & 2	505–530(1&2),535–575(1),660–710(1), 740–750(1),752–762(1,2),770–860(1), 880–900(1),912–923(1),960–995(1)		
	cattail	1 & 2	505–520(1,2),605–620(2),623–633(1,2), 670–700(2),920–935(1)		
	pl	2	505–520,905		
09-September	reed	1,2,3	520–535,540–560 580–585		
	pl	2	690–704		
18-September	reed	1 & 2	650–680,720–740,746–755,765, 910–920,922–935		
	cattail	1 & 2	650–680,720–740,746–755,765, 910–920,922–935	965	
23-September	reed	3	520–530,560–575,630–650,700–720, 740–750,755–765,770–810,830–920, 930–940,950–970		
	pl	1	515–530,580–590,655–665(2), 665–670, 678–698(1,2), 965		
30-September	reed	1,2,3	625,805		
	cattail	1	540–555,590–620,640–675,690		
	pl	1	505–535,(1,2,3), 535–592, 625–640(1,2,3), 655–680(2), 660–680(1,3), 928–960(2), 675,695–700,750, 935–970(3)		
07-October	cattail	1,2,3	665–670		
	pl	1 & 3	675–700(1,3)		
15-October	reed	1 & 3	500–525,570,620,635,745,755,920		
	cattail	1	670		

in detail to identify spectral ranges in which one or more community types have distinguishing features. Experimental results, illustrated in Figures 3 to 5 and are summarized in Table 2, suggest that six dates, between 15 July and 30 September, offered the highest potential for differentiation among community types. Optimal differentiability occurred on 30 August, when the three community types (reed-, cattail, and loosestrife-dominated) could be discriminated completely in the spectral range 680 *n*m to 740 *n*m typically associated with the "red edge", which other authors have also found to be diagnostic of plant community types and environmental conditions. The date of 30 August

corresponds to a time of significant changes in the phenology of the targeted wetland plants, in particular the progressive replacement of flowers by seed heads and the preferential growth of reed plants relative to other plants in the wetlands.

Now that the present, preliminary study has determined the time of year that appears optimal for the discrimination of wetland plant community types using DSA, the next step of the research would be to perform a land cover classification on hyperspectral images of selected wetland areas acquired in late August. Spectral derivatives in a number of training sites could be compared and provide information on whether the spectral ranges identified in the present article would once again allow discrimination among community types, or whether other spectral ranges would be preferable. To achieve this objective, several improvements and extensions to the approach developed in this research would be worthwhile. In particular, a computer program could be developed to replace the visual inspection. Finally, an additional area for further research would be to compare and contrast the DSA method with other techniques that have been used to map invasive species, e.g., the continuum removal of key areas of the spectrum.

Acknowledgments

The research reported in this article was supported by the Hudson River Estuary Program, New York State Department of Environmental Conservation. The authors also acknowledge with gratitude the thorough comments of the three anonymous reviewers.

References

Adams, M.L., W.D. Philpot, and W.A. Norvell, 1999. Yellowness index: An application of spectral second derivative to estimate chlorosis of leaves in stressed vegetation, *International Journal of Remote Sensing*, 20(18):3663–3677.

Armstrong, D.W., 1979. Aerial infrared imagery of leafy spurge (*Euphorbia esula*), *Proceedings of the Leafy Spurge Symposium*, 26–27 June 1978, Bismark, North Dakota, pp. 68–69.

Bachmann, C.M., T.F. Donato, G.M. Lamella, W.J. Rhea, M.H. Bettenhausen, R.A. Fusina, K.R. DuBois, J.H. Porter, and B.R. Truitt, 2002. Automatic classification of land cover on Smith Island, VA, using HyMAP imagery, *IEEE Transactions on Geoscience and Remote Sensing*, 40(10):2313–2330.

Byers, J.E., S. Reichard, J.M. Randall, I.M. Parker, C.S. Smith, W.M. Lonsdale, I.A.E. Atkinson, T.R. Seastedt, M. Williamson, E. Chornesky, and D. Hayes, 2002. Directing research to reduce the impacts of nonindigenous species, *Conservation Biology*, 16(3):630–640.

Chang, C.I., Q. Du, T. Sun, and M.L.G. Althouse, 1999. A joint band prioritization and band-decorrelation approach to band selection for hyperspectral image classification, *IEEE Transactions Geoscience and Remote Sensing*, 37(6):2631–2641.

Clark, C.D., P.J. Mumby, J.R.M. Chisholm, J. Jaubert, and S. Andrefouet, 2000. Spectral discrimination of coral mortality states following a severe bleaching event, *International Journal of Remote Sensing*, 21(11):2321–2327.

Cole, N.B., and E. Fried, 1981. *Freshwater Wetlands Inventory*, Division of Fish and Wildlife, New York State Department of Environmental Conservation.

Demetriades-Shah, T. H., Steven, M.D., and J.A. Clark, 1990. High resolution derivatives spectra in remote sensing, *Remote Sensing of Environment*, 33:55–64.

Everitt, J.H., G.L. Anderson, D.E. Escobar, M.R. Davis, N.R. Spencer, and R.J. Andrascik, 1995. Use of remote sensing for detecting and mapping leafy spurge (*Euphorbia esula*), *Weed Technology*, 9:599–609.

Frazier, B.E., and B.C. Moore, 1993. Some tests of film types for remote sensing of purple loosestrife, *Lythrum salicaria*, at low densities, *Wetlands*, 13:145–152.

Fung, T., F.Y. Ma, and W.L. Siu, 2001. Subtropical tree recognition with hyperspectral data analysis in Hong Kong, *Geocarto International*, 16(3):25–34.

Gleason, H.A., A. Cronquist. 1991. *Manual of vascular plants of northeastern United States and adjacent Canada*, Second edition, New York Botanical Garden, New York, USA.

Green, A.A., M. Berman, P. Switzer, and M.D. Craig, 1988. A transformation for ordering multispectral data in terms of image quality with implications for noise removal, *IEEE Transactions on Geoscience and Remote Sensing*, 26:65–74.

Hanlon, C., 1995. Vegetation Mapping (GIS) and Management in Lake Okeechobee, Florida, USA, *Lake and Reserve Management*, 11(2):147.

Harsanyi, J.C., and C. Chang, 1994. Hyperspectral image classification and dimensionality reduction: An orthogonal subspace projection approach, *IEEE Transactions on Geoscience and Remote Sensing*, 32:779–785.

Hirano, A., 2000. Suitability of hyperspectral image data for wetland vegetation mapping, *Proceedings of the ASPRS 2000 Annual Convention*, 22–26 May, Washington, D.C., American Society for Photogrammetry and Remote Sensing, Bethesda, Maryland, unpaginated CD-ROM.

Holroyd, E. W III., and D. Eberts. 2000. *Aerial documentation of effective biocontrol of purple loosestrife at Winchester Wasteway*, Riparian Ecology and Management in Multi-Land Use Watersheds, American Water Resources Association (Wigington and Beschta, editors). Washington, D.C.

IPC of NYS, 2005. URL: http://www.ipcnys.org (last date accessed: 22 February 2005).

Juan, C.H., J.D. Jordan, and C.H. Tan. 2000. Application of airborne hyperspectral imaging in wetland delineation, *Proceedings of the Asian Conference in Remote Sensing (ACRS)*, 04–08 December, Taipei, Taiwan, URL: http://www.gisdevelopment.net/aars/acrs/2000/ts16/hype0006.shtml (last date accessed: 22 February 2005).

Juan, C.H., and S.F. Shih. 1997. A lysimeter system for evapotranspiration estimation for wetland vegetation, *Proceedings of the Soil and Crop Scoiety of Florida*, 56:125–130.

Lee, J.B., A.S. Woodyatt, and M. Berman. 1990. Enhancement of high-spectral resolution remote-sensing data by a noise-adjusted principle components transform, *IEEE Transactions on Geoscience and Remote Sensing*, 28:295–304.

Mathworks, Inc., 2005. MATLAB Toolbox, URL: http://www.mathworks.com (last date accessed: 22 February 2005).

McCormick, C.M., 1999. Mapping Exotic Vegetation in the Everglades using large-scale aerial photographs, *Photogrammetric Engineering & Remote Sensing*, 65(2):179–184.

Nellis, M.D., and Y. Tao, 1999. Reflectance heterogeneity in a tallgrass prairie national preserve based on ground based measurement, Proceedings of the American Society of Photogrammetry and Remote Sensing Annual Meeting, pp. 491–497.

Ocean Optics, Inc., 2005. URL: http://www.oceanoptics.com (last date accessed: 22 February 2005).

Philpot, W.D., M. Kim, and F. Tsai, 1997. Analysis of hyperspectral data for detailed water quality information, *Proceedings of the 4th International Conference on Remote Sensing of Coastal and Marine Environments*, 17–19 March, Orlando, Florida.

Philpot, W.D., and D.D. Kohler, 1999, Deriving bathymetry from hyperspectral data, *IUGG '99, IAPSO Symposium P15: Optical Oceanography & UV Radiation, Birmingham, U.K.*

Philpot, W.D, M. Duggin, R. Raba, and F. Tsai, 1996. Analysis of reflectance and fluorescence spectra for a typical features: Fluorescence in the Yellow-Green, *Plant Physiology*, 148: 567–573.

Qingxi, T., Z. Lanfen, W. Jinnian, and Z. Bing, 1997. Study on the wetland environment by airborne hyperspectral remote sensing, *Third International Airborne Remote Sensing Conference and Exhibition*, 07–10 July, Copenhagen, Denmark.

Rowlinson, L.C., M. Summerton, and F. Ahmed, 1999. Comparison of remote sensing data sources and techniques for identifying and classifying alien invasive vegetation in riparian zones, *Water SA*, 25(4):497–500.

Spencer, N.R., 1999. *Proceedings of the X International Symposium on Biological Control of Weeds*, 04–14 July, Bozeman, Montana.

Spanglet, H.J., S.L. Ustin, and E. Rejmankova, 1998. Spectral Reflectance characteristics of California subalpine marsh plant communities, *Wetlands*, 18(3):307–319.

Splajt, T., G. Ferrier, and L.E. Frostick, 2003. Monitoring of landfill leachate dispersion using reflectance spectroscopy and ground-penetrating radar, *Environmental Science and Technology, 37:4293–4298*.

Staenz, K., 1996. Classification of a hyperspectral agricultural dataset using band moments for reduction of the spectral dimensionality, *Canadian Journal of Remote Sensing*, 22(3): 248–257.

Stein, B.A., and S.R. Flack, editors, 1996. *America's Least Wanted: Alien Species Invasions of U.S. Ecosystems*, The Nature Conservancy, Arlington, Virginia.

Thenkabail, P.S., R.B. Smith, and E. De Pauw, 2002. Evaluation of narrowband and broadband vegetation indices for determining optimal hyperspectral wavebands for agricultural crop characterization, *Photogrammetric Engineering & Remote Sensing*, 68(6):607–621.

Thompson, D.Q., R. Stuckey, and E.B. Thompson. 1987. *Spread, impact, and control of purple loosestrife (Lythrum salicaria) in North American wetlands*, United States Department of the Interior, Fish and Wildlife Service, Washington, D.C.

Tiner, Jr., R.W., 1987. *A field guide to coastal wetland plants of the Northeastern United States*, The University of Massachusetts Press, Amherst, Massachusetts, 285 p.

Tsai, F., and W.D. Philpot, 1998. Derivative analysis of hyperspectral data, *Remote Sensing of Environment*, 66(1):41–51.

Tsai, F., and W.D. Philpot, 2002. A Derivative-aided image analysis system for land-cover classification, *IEEE Transactions on Geoscience and Remote Sensing*, 40(2):416–425.

Underwood, E., S. Ustin, and D. DiPietro, 2003. Mapping noninvasive plants using hyperspectral imagery, *Remote Sensing of Environment*, 86:150–161.

Williams, A.P., and E.R. Hunt, Jr., 2002. Estimation of leafy spurge cover from hyperspectral imagery using mixture tuned matched filtering, *Remote Sensing of Environment*, 82:446–456.

(Received 08 December 2003; accepted 27 February 2004; revised 23 March 2004)